Cancer Cell International

RESEARCH Open Access

# Curcumin blunts epithelial-mesenchymal transition to alleviate invasion and metastasis of prostate cancer through the JARID1D demethylation

Qinghua Xie[1,2†], Yaohua Hu[1†], Chenyang Zhang[1,3†], Caiqin Zhang[1], Jing Qin[1], Yong Zhao[1], Qingling An[1], Jie Zheng[4] and Changhong Shi[1*]

**Abstract**

Prostate cancer (PCa) is one of the most common and prevalent cancers in men worldwide. The majority of PCa-related deaths result from metastasis rather than primary tumors. Several studies have focused on the relationship between male-specific genes encoded on the Y chromosome and PCa metastasis; however, the relationship between the male specific protein encoded on the Y chromosome and tumor suppression has not been fully clarified. Here, we report a male specific protein of this type, the histone H3 lysine 4 (H3K4) demethylase JARID1D, which has the ability to inhibit the gene expression program related to cell invasion, and can thus form a phenotype that inhibits the invasion of PCa cells. However, JARID1D exhibits low expression level in advanced PCa, and which is related to rapid invasion and metastasis in patients with PCa. Curcumin, as a multi-target drug, can enhance the expression and demethylation activity of JARID1D, affect the androgen receptor (AR) and epithelial-mesenchymal transition (EMT) signaling cascade, and inhibit the metastatic potential of castration resistant cancer (CRPC). These findings suggest that using curcumin to increase the expression and demethylation activity of JARID1D may be a feasible strategy to inhibit PCa metastasis by regulating EMT and AR.

## Introduction

PCa is the second leading cause of cancer-related mortality among men, highlighting its prevalence and global health impact [1]. While androgen deprivation therapy for advanced PCa initially exerts excellent anticancer effects [2], the majority of patients eventually progress to androgen-resistant PCa, termed castration-resistant prostate cancer (CRPC). This type of PCa displays stronger invasion and metastasis abilities, with no effective treatment option currently available. A substantial proportion of CRPC patients may further progress to metastatic CRPC, exhibiting a diverse spectrum of molecular tumor characteristics and varying degrees of progression risk, as indicated by recent studies [3]. This may rapidly develop into a phenotype similar to lethal neuroendocrine prostate cancer (NEPC) [4]. Therefore, it is of great significance to explore the molecular mechanisms underlying PCa metastasis and develop novel therapeutic strategies to prevent the progression of PCa.

Several studies have focused on the relationship between male-specific genes encoded on the Y

†Qinghua Xie, Yaohua Hu and Chenyang Zhang contributed equally to this work.

*Correspondence:
Changhong Shi
changhong@fmmu.edu.cn

Full list of author information is available at the end of the article

**Graphical abstract**

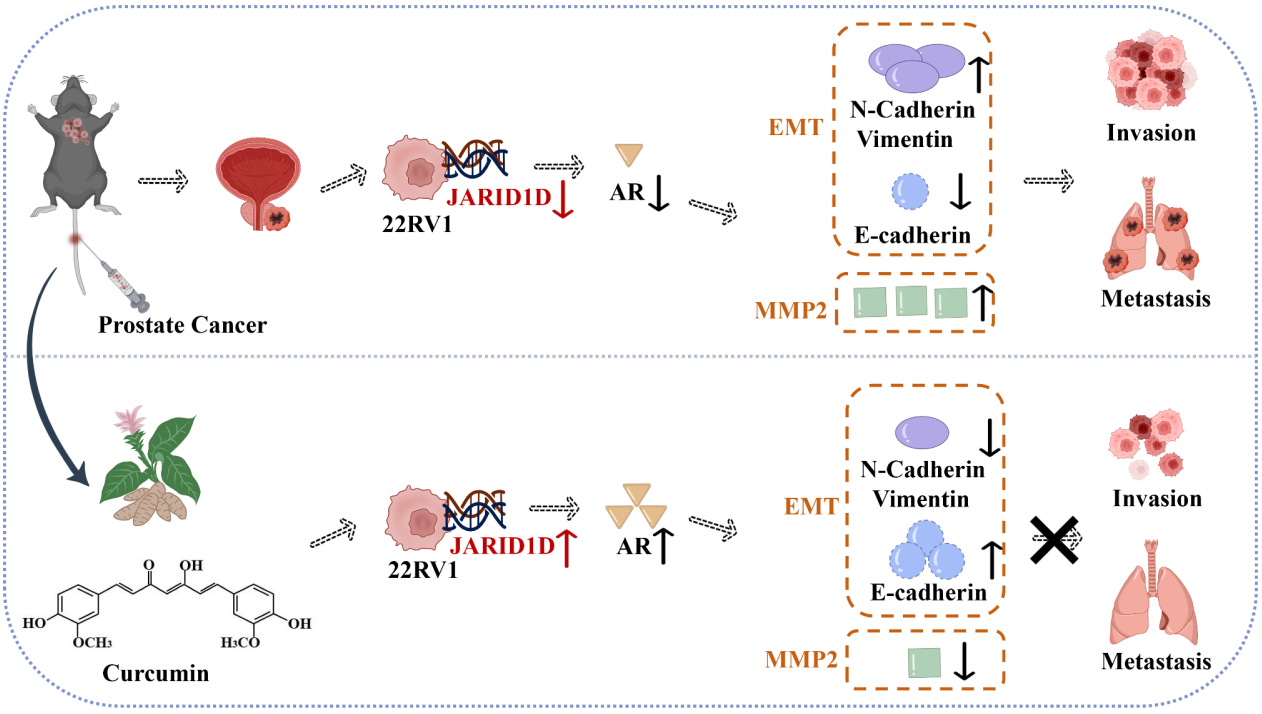


## Highlights

- Knockdown of JARID1D can enhance the invasion and metastasis ability of prostate cancer cells.
- Curcumin improves the expression and demethylation activity of JARID1D.
- Curcumin can stimulate the JARID1D/AR/EMT signaling cascade through demethylation to inhibit the metastatic potential of castration-resistant prostate cancer.

**Keywords** JARID1D, Metastasis, Curcumin, Demethylase, Prostate cancer

chromosome and PCa [5]. A male-specific protein encoded on the Y chromosome, histone H3 lysine 4 (H3K4) demethylase JARID1D (also called KDM5D and SMCY), has the ability to inhibit gene expression programs related to cell invasion. Li et al. [6] reported that the expression level of JARID1D in patients with metastatic PCa is very low, occasionally being undetectable. Knockdown of JARID1D in NEPC cells with reduced or lost reliance on the androgen receptor (AR) can enhance their metastatic ability, and overexpression of JARID1D can inhibit their invasive ability [6]. JARID1D specifically represses invasion-associated genes. High heterogeneity is a pivotal clinical characteristic of PCa, wherein the role of AR as an initiating factor driving the high heterogeneity of PCa in JARID1D driven metastasis is unclear. Taken together, these findings provide evidence that JARID1D may be an anti-invasion target for suppressing PCa progression. However, it is still challenging to develop specific targeting agonists to activate JARID1D, which suggests that we may need to explore drugs with multi-target pharmacodynamic relationships, exemplified by the herbal compound curcumin. In view of the role of JARID1D in tumor development and the pleiotropic effect of curcumin, taking curcumin or its derivatives as potential candidates to regulate JARID1D activity may improve the expression of JARID1D and play an anti-tumor role.

Curcumin, fundamentally a polyphenolic compound, is derived as a powder from the rhizome of the perennial herb, Curcuma longa [7]. Previous studies have shown that curcumin, as a multi-target drug, has anti-inflammatory, antioxidant, anti-infective, anti-fibrotic, and anti-atherosclerotic properties, which could significantly inhibit the occurrence and metastasis of various malignant tumors [8]. In addition, mounting evidence indicates that curcumin can act as an epigenetic regulator to exert anti-tumor effects [9]. For example, it can improve the expression of histone deacetylases, DNA methyltransferases, and inhibit the invasion and migration of tumors [10, 11]. However, the epigenetic mechanism of curcumin preventing PCa metastasis has not been fully clarified. Despite these advances, the precise

epigenetic mechanism through which curcumin forestalls PCa metastasis remain to be comprehensively elucidated.

In this study, CRPC cells were treated with curcumin, and the changes in cell morphology, proliferation, and gene methylation status were analyzed to determine the changes in JARID1D methylation. We further examined AR expression and EMT-related molecules. The results demonstrated that the invasion and metastasis of PCa induced by the knockdown of JARID1D were significantly inhibited by curcumin. Curcumin inhibits the metastatic potential of CRPC cells by regulating AR and EMT-related genes through methylation of JARID1D. These results underscore the therapeutic potential of curcumin in the treatment of invasive prostate cancer.

## Materials and methods

### Cell culture

The PCa cell lines LNCaP, C4-2, PC3, DU145, $C42^R$ (20 μm of Enzalutamide induced for 120 days) and 22Rv1 were obtained from the American Type Culture Collection (Manassas, VA, USA) and cultured in RPMI 1640 medium with 10% fetal bovine serum (Gibco Cat# 10099141 C) at 37 °C and 5% $CO_2$. All the cell cultures contained 1% penicillin and 1% streptomycin (Gibco Cat# 1037801). When the cell density reached 80-90%, 0.25% trypsin was used for sub-culturing.

### Chronic virus transfection assays

The day before transfection, 22RV1 cells with good cell status were inoculated in the 6-well plate, and the confluent degree reached 30-50% the next day. Transfection was performed with a special transfection reagent polybrene, followed by a system of 2 mL culture medium per well, 2.5 μL polybrene and 10 μL disease venom. Fresh culture medium was replaced 4–6 h after transfection. After 48 h, the transfection efficiency was verified by RT-PCR and Western blot. When the mRNA and protein expression levels of JARID1D were significantly reduced, it was confirmed that the stable lentivirus strain was successfully constructed.

### RT-PCR assays

A total RNA extraction kit was used to extract the total RNA of each group of cell samples, and a reverse transcription kit was used to reverse-transcribe RNA into cDNA. The reaction conditions were 37 °C for 15 min and 85 °C for 15 s. Then real-time fluorescent quantitative PCR was conducted on the cDNA of each group of samples. With β-Actin is an internal reference gene, Formula $2^{-\Delta\Delta CT}$ calculates the relative expression levels of each group of genes. The reagents and instruments used were PrimeScript™ RT Reagent Kit, TB Green® Fast qPCR Mix (Takara, Beijing, China), Step One Plus real-time PCR Detection System (Applied Biosystems, Thermo Fisher, Waltham, MA, USA). PCR reaction conditions were set as follows: predenaturation at 95 °C for 30 s, PCR at 95 °C for 15 s, and PCR at 60 °C for 30 s for 40 cycles. The primer sequences used for PCR are listed in Supplementary Table 1.

### Western blot analysis

According to the experimental protocol reported in the literature [12], the protein was extracted from the cells with lysate, and the protein concentration was determined with BCA protein quantitative kit. Then, 10% SDS-PAGE gel was assembled, gel electrophoresis was performed, and proteins were separated according to molecular weight. Electrophoresis conditions: 90 V, 400 mA, 120 min. The transfer box was assembled with the gel closest to the negative electrode and the film closest to the positive electrode. Transfer condition: 90 V, 400 mA, time depends on the size of the molecular weight. After the transfer, the PVDF membrane was soaked in 5% skim milk powder for 2 h. The membrane was incubated with a primary antibody against the target protein, and shaken gently overnight at 4 °C, or incubated at room temperature for 1 h. Finally, an imaging system was used to capture and analyze the images, and the protein antibodies used in the experiment were: JARID1D (Affinity Biosciences, DF2548, 1: 1000), AR (Abcam, ab108341, 1:1000), N-cadherin (United Kingdom, Abcam, ab76011, 1:1000), E-cadherin (Proteintech, 20874-1-AP, 1:1000), MMP2 (United Kingdom, Abcam, ab92536, 1:1000), H3K4me3 (Affinity, DF6935, 1:1000), Vimentin (Proteintech 10366-1-AP, 1:1000) and β-actin (Engibody, AT0001, 1:2000).

### Transwell assay

The 22RV1 sh-JARID1D cells were established *via* the transfection of chronic viruses to knock down JARID1D expression; 22RV1-NC cells were the corresponding controls. These cells were added to the chamber and cultured for 48 h. The cells were then fixed with 4% paraformaldehyde and stained with crystal violet, and the microscope was used to capture the images of the cells passing through the Transwell chamber.

### Animal experiment

Male BALB/c nude mice, aged 6–7 weeks, were sourced from GemPharmatech Co. Ltd. (Chengdu, China) and housed in a pathogen-free environment at the Laboratory Animal Center of the Fourth Military Medical University (FMMU). Our animal study protocol was meticulously reviewed and approved by the Institutional Review Board of the Institutional Animal Care and Use Committee of FMMU (Protocol code: No. 20200417, approved on March 20, 2020), ensuring all procedures adhered to the highest ethical standards.

In our study, $2\times10^6$ 22RV1 sh-JARID1D and $2\times10^6$ 22RV1-NC cells were injected into the tail veins of the mice. To monitor metastasis in vivo, small-animal optical imaging was employed using the Caliper Lumina II system after a 4-week observation period. Lung tissue sections were subsequently harvested for histological examination *via* H&E staining upon detection of metastatic signals.

For the curcumin intervention experiments, $2\times10^6$ 22RV1 sh-JARID1D cells labeled with luciferase were similarly injected. After a 4-week establishment period, mice were randomly assigned to two groups ($n=7$ per group) in a blinded manner, ensuring equal distribution of baseline characteristics. The treatment group received intraperitoneal injections of curcumin (Selleck, USA, S1848) at a dosage of 30 mg/kg body weight, administered biweekly, while the control group received equivalent volumes of the vehicle. Body weight was closely monitored throughout the study to assess general health. Bioluminescence imaging was conducted weekly for 3 weeks using the Xenogen IVIS50 imaging system, with the following parameters: field of view set to 'D', binning at '4' for optimal signal-to-noise ratio, exposure time adjusted based on initial pilot scans to maximize the dynamic range without saturation, and f/stop at '1' for maximum light collection. Signal quantification was performed using Living Image 4.7.3 software, applying a standardized protocol for region of interest (ROI) identification and quantification. We defined metastatic signals as any ROI with a total flux exceeding a threshold of $1\times10^6$ photons/second. Upon completion of the study, mice were humanely euthanized, and lung tissues were collected for paraformaldehyde fixation, ensuring rigorous adherence to our predefined monitoring protocols and ethical considerations.

#### Methylation specific PCR (MSP)

Genomic DNA was extracted using proteinase K digestion and phenol/chloroform extraction, which was quantified using an ultraviolet spectrophotometer and stored at −20 °C. DNA was purified using a Wizard clean-up system kit (Takara, Beijing, China), and the specific steps were carried out according to the manufacturer's instructions. DNA bisulfite modification was performed using standard protocols [13]. The detailed procedure involved initial denaturation at 99 °C for 10 min, followed by incubation at 50 °C for 60 min with intermittent mixing, and a final cooling step at room temperature for 10 min. After 24 h of culture, the methylation status of the cells in each group was detected by the MSP method [14]. The MSP primer sequences, annealing temperatures, and fragment sizes of JARID1D are listed in Supplementary Table 2.

#### Cell viability analysis

According to the product manual provided by the manufacturer, cell samples were collected and Cell Count Kit-8 (7 Sea Biotech, Shanghai, China) was used to determine their growth activity. Tumor cells were cultured in 96-well plates ($3\times10^3$ cells/well), and curcumin was added at varying concentrations. Following a 72-hour incubation, 100 μL medium-CCK-8 mixture at a ratio of 9:1 was added and incubated for 2 h. Absorbance values were measured at 450 nm, and cell viability was calculated based on these values. Finally, use GraphPad software, select normalized Response Variable slope, perform curve fitting, and obtain its IC50 value. The relevant data are listed in Supplementary Table 3.

#### ChIP assay

ChIP assays were determined with the Simple ChIP Plus Enzymatic Chromatin IP Kit (Cell Signaling Technology, 91820). A total of $7.5\times10^6$ cells were cross-linked at room temperature for 10 min using a 1% solution of paraformaldehyde. The cross-linking reaction was quenched by adding 1 mL of 1.25 M glycine and incubating for 5 min. The cross-linked chromatin was subsequently transferred to AFA fiber tubes (Covaris) and sonicated to achieve an average fragment size of 150–200 base pairs (bp) in a 0.2% SDS shearing buffer using a Covaris sonicator. The sonicated chromatin was centrifuged at 13,000 rpm for 5 min and diluted to a final concentration of 0.1% SDS. The chromatin was pre-cleared using Dynabeads Protein G (Life Technologies) for 1 h. Chromatin-protein complexes were then immunoprecipitated with 5 μm of specific antibodies at 4 °C overnight. On the subsequent day, Dynabeads Protein G were added again for a 2-hour incubation. The beads were thoroughly washed with a series of buffers: low-salt wash buffer, high-salt wash buffer, LiCl wash buffer, and finally with TE buffer. The precipitated chromatin was eluted from the beads using 300 μL of elution buffer (1% SDS, 0.1 M $NaHCO_3$) for 1 h at room temperature, followed by de-cross-linking at 65 °C overnight. The ChIP and input DNA samples were treated with RNase A and proteinase K, and then extracted using phenol-chloroform extraction. The integrity and size of the DNA fragments (150–200 bp) were assessed using a High Sensitivity DNA Kit on an Agilent 2100 Bioanalyzer. The antibodies used in the experiment were: anti-AR (Cell Signaling Technology, 5153), anti-JARID1D (Affinity Biosciences, DF2548), and anti-H3K4me3 (Abcam, ab6002) antibodies. In addition, anti-histone H3 antibodies (Cell Signaling Technology, 4620) and normal rabbit IgG antibodies (Cell Information Technology, 2729) were used as positive and negative control groups, respectively. Finally, to analyze the DNA derived from ChIP, quantitative RT-PCR was used. For the quantitative RT-PCR analysis, we used SYBR Green

Master Mix and specific primers designed to amplify ROIs. The PCR program included an initial denaturation step at 95 °C for 10 min, followed by 40 cycles of 95 °C for 15 s and 60 °C for 1 min. Data were normalized to input DNA and expressed as fold enrichment relative to a negative control region. The relevant primers are listed in Supplementary Table 1.

#### Co-immunoprecipitation (Co-IP)

For Co-IP, we prepared $8\times10^6$ cells and lysed them in lysis buffer containing 10 mM Hepes-NaOH (pH 8), 1.5 mM $MgCl_2$, 25% glycerol, 0.5% Nonidet P-40, 0.42 M NaCl, 0.2 mM EDTA, and 0.5 mM DTT. After centrifugation at 13,200 rpm for 10 min, diluted in a dilution buffer (20 mM Tris-HCl, pH 8.0, 1.5 mM $MgCl_2$, 0.2 mM EDTA, 0.5% Nonidet P-40), and supplemented with 3 mM $MgCl_2$ and 20 U/mL DNase (NEB). The mixture was incubated at 37 °C for 30 min. To preclear the lysate, 30 µL of Dynabeads Protein G (Life Technologies) were added and incubated at 4 °C for 60 min with gentle rotation. Subsequently, 10% of the lysate was reserved as the input control, and the remainder was incubated with 5 µg of the following primary antibodies overnight at 4 °C: JARID1D (Affinity Biosciences, DF2548, 5 µg/µL), AR (Cell Signaling Technology, 5153, 5 µg/µL), IgG (SC-2027, 2 µg/µL). On the following day, 50 µL of Dynabeads Protein G were added to the lysate and incubated for 2 h at 4 °C with gentle rotation. The precipitated proteins were then washed twice with a low-salt Co-IP wash buffer (20 mM Tris-HCl, pH 8.0, 150 mM NaCl, 1.5 mM $MgCl_2$, 0.5% Nonidet P-40, 0.2 mM EDTA). Finally, 30 µL of NuPAGE LDS sample buffer with DTT (Bio-Rad) was added to the beads, and the mixture was heated at 95 °C for 5 min. The supernatants were then subjected to immunoblotting to detect the proteins of interest.

#### Immunohistochemistry (IHC)

The process began with tissue sectioning and preparation, followed by deparaffinization and antigen retrieval to expose antigenic sites. Endogenous peroxidase was blocked, and non-specific binding was prevented with serum blocking. The sections were then incubated with a primary antibody to target the protein of interest, followed by an enzyme-conjugated secondary antibody. After washing, a chromogenic substrate was applied for signal development, typically resulting in a colored reaction product at the antigen location. The sections were counterstained, dehydrated, and mounted for microscopic analysis to assess protein presence and distribution. IHC analysis was performed using antibodies against JARID1D (USA, Affinity Biosciences, DF2548, 1:100), AR (United Kingdom, Abcam, ab108341, 1:200), E-cadherin (Proteintech, 20874-1-AP, 1:5000), N-cadherin (United Kingdom, Abcam, ab76011, 1:200), MMP2 (United Kingdom, Abcam, ab92536, 1:100), Vimentin (Proteintech, 10366-1-AP, 1:3000) and CK8 (United Kingdom, Abcam, ab53280, 1:250).

#### H&E staining

H&E staining is a commonly used histological technique in pathology for evaluating the morphological characteristics of tissue sections. In our study, tissue sections were first subjected to fixation, followed by hydration. They were then stained with hematoxylin to color the cell nuclei. After staining, the sections were rinsed with water and subsequently stained with eosin to color the cytoplasm and other tissue structures. Once the staining process was complete, the sections were dehydrated through a series of gradually increasing concentrations of alcohol, ultimately clearing away excess dye and undergoing clarification treatment. Finally, the sections were mounted in a resin medium to protect the staining and were observed and analyzed under a light microscope.

#### Statistical analysis

The data are presented as mean±standard error (SE), and were analyzed using GraphPad Prism (GraphPad Software, San Diego, USA). Differences between experimental groups were tested using the Student's *t*-test and one-way and two-way analysis of variance (ANOVA) ($P<0.05$).

## Results

#### Knockdown of JARID1D enhances the invasive ability of PCa cells

To explore the relationship between JARID1D and the invasion of PCa cells, a cell line with JARID1D knockdown was established. First, the expression of JARID1D in five PCa cell lines (22RV1, LNCaP, PC3, C4-2 and DU145) was detected using RT-PCR and western blot. The experiments of Western blot (Fig. 1A) and RT-PCR (Fig. 1B) confirmed that JARID1D was highly expressed in 22RV1 cells. Meanwhile, 22RV1 cells represented the most common cell types that underwent metastasis in clinic with the characteristics of CRPC. This cell line also displayed certain metastatic potential in transplanted tumor models. For these reasons, we chose 22RV1 cells for this study. Three siRNAs (si-1, si-2 and si-3) were designed to transfect 22RV1. Then, the results from both RT-PCR and Western blot analyses indicated that, compared to the control group (si-nc), the knockdown effect of si-1 was the most pronounced. (Supplementary Fig. 1). Therefore, the si-1 sequence packaging was selected for the synthesis of chronic viruses. Western blot and RT-PCR showed that compared to 22RV1-NC, the protein and mRNA expression levels of JARID1D were both reduced, suggesting that the stable cell line with low expression of JARID1D has been successfully

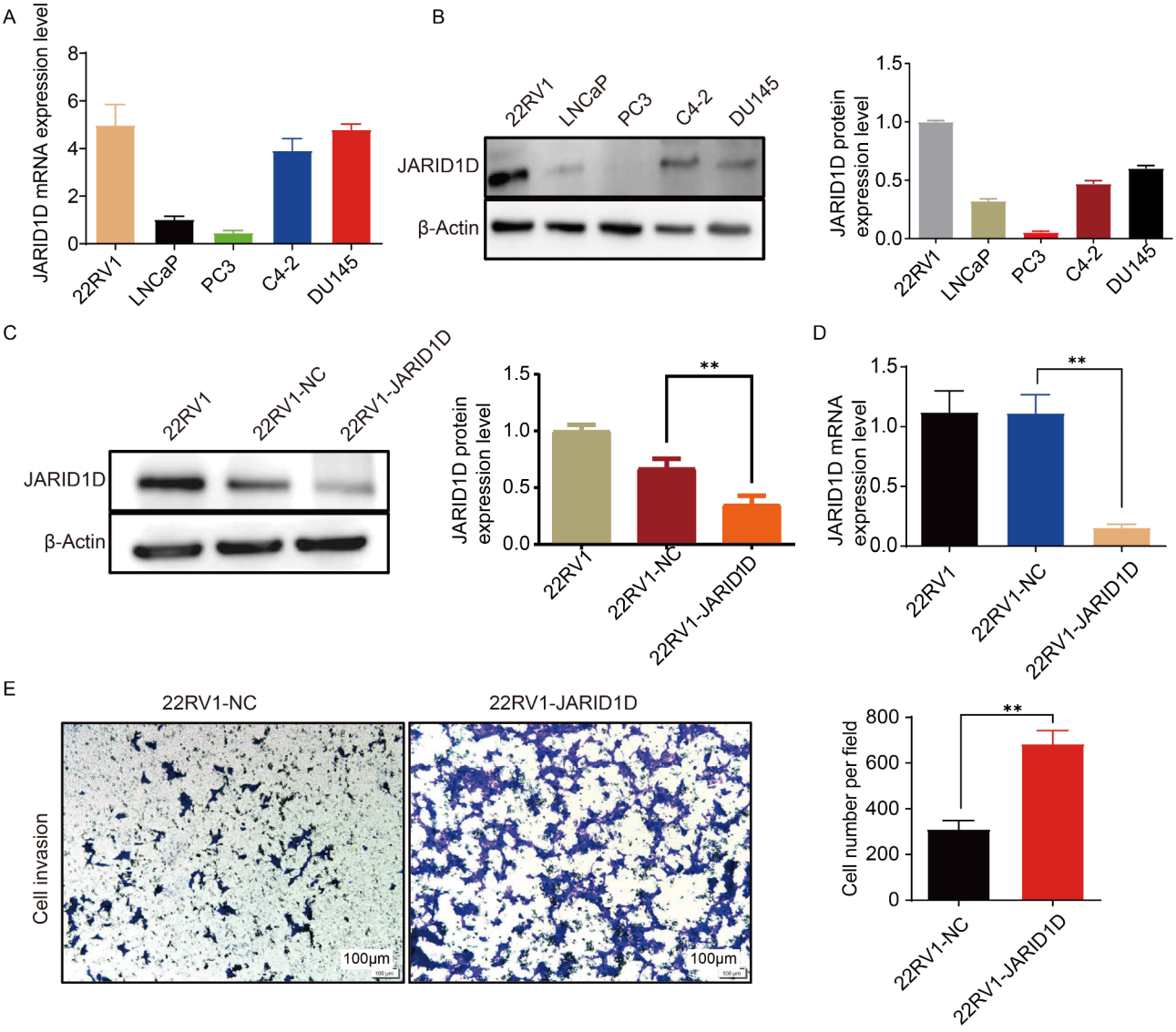


**Fig. 1** Knocking down JARID1D can enhance the invasive ability of PCa cells. (**A-B**) The expression of JARID1D in PCa cell lines (22RV1, LNCaP, PC3, C4-2 and DU145) was analyzed using quantitative RT-PCR (**A**) and Western blot (**B**) and quantitative analysis results. (**C-D**) The expression of JARID1D after 22RV1 cells transfection into lentivirus was analyzed using Western blot and quantitative analysis results. (**C**) and quantitative RT-PCR (**D**). (**E**) Transwell (left) and its quantification (right) analyzed the changes in the invasion ability of the 22RV1 cells after knockdown of JARID1D when compared with the NC group, *$P<0.05$, **$P<0.01$, ***$P<0.001$. PCa, prostate cancer; NC, normal control

constructed. (Figure 1C and D). Furthermore, Transwell experiments showed that the invasion ability of 22RV1 ($P<0.01$) cells was significantly enhanced after knockdown of JARID1D (Fig. 1E). This suggested that JARID1D could regulate PCa cell invasion and might be an epigenetic inhibitor of PCa cell invasion.

### Knockdown of JARID1D promotes metastasis of PCa in a xenograft model

To evaluate the effect of JARID1D on the metastasis of PCa cells in vivo, we established a lung metastasis xenograft model through tail vein injection of PCa cells into nude mice and dynamically monitored the metastasis of the tumor cells using small-animal optical imaging. Four weeks after tumor cell injection, the luciferase signals in 22RV1 sh-JARID1D ($P<0.01$) mice were significantly higher than those in the 22RV1-NC mice (Fig. 2A), and the metastatic signal was mainly concentrated in the lungs (Fig. 2B). At the end of the experiment, the mice were euthanized and the lung tissues were dissected. After fixation and paraffin embedding, H&E staining confirmed that the number of tumor metastatic lesions in the 22RV1 sh-JARID1D group was significantly higher than that in the 22RV1-NC group (Fig. 2C). These results indicated that the knockdown of JARID1D could promote the metastatic ability of 22RV1 cells in vivo.

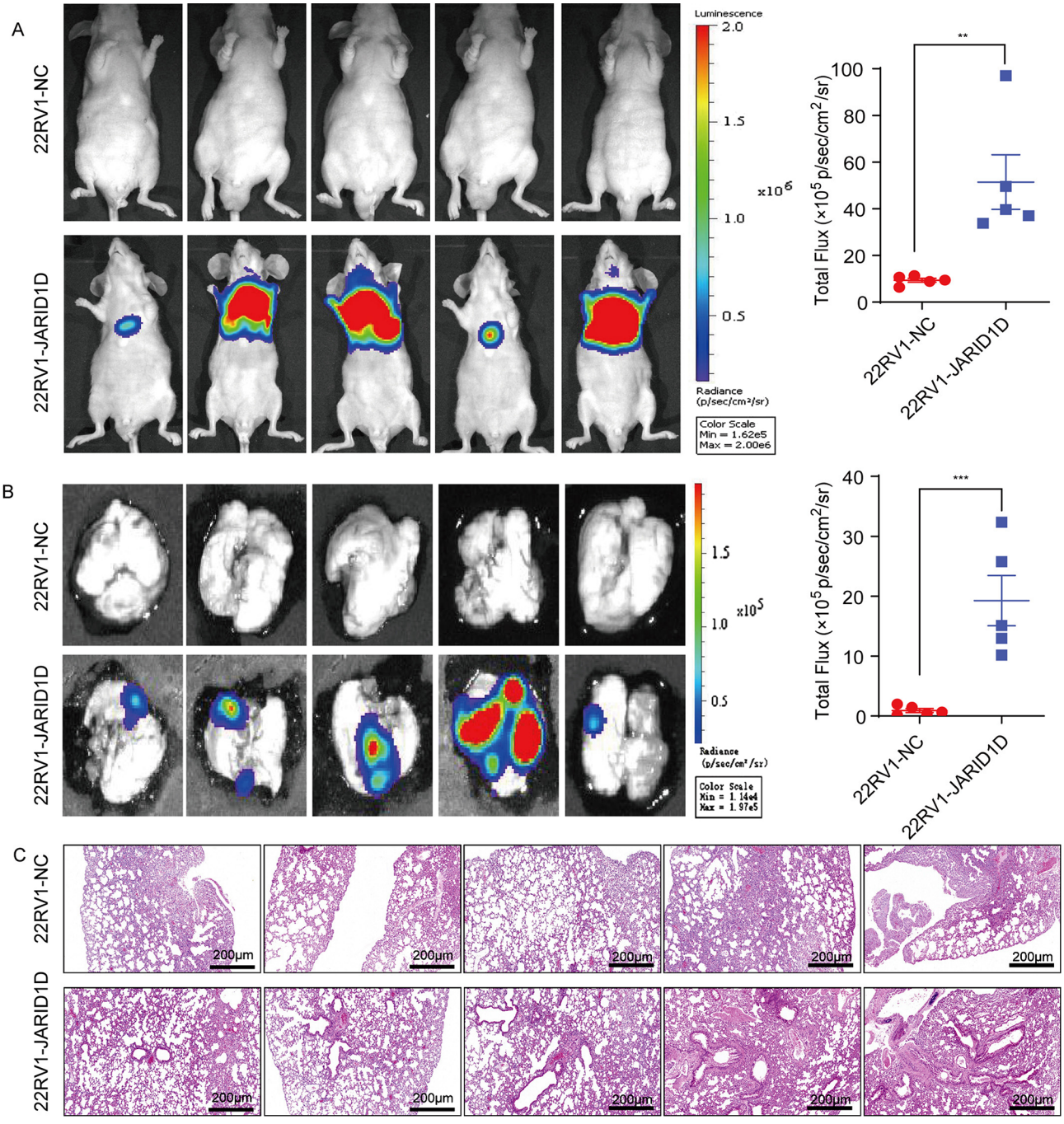


**Fig. 2** Knocking down JARID1D promotes the metastasis of prostate tumor cells in vivo. Lung metastasis xenograft model was established through tail vein injection of 22RV1 cells into nude mice. (**A-B**) Bioluminescence image (left) and its quantification (right) of (**A**) whole mouse and (**B**) mouse lung tissue after knockdown of JARID1D in the 22RV1 cells. (**C**) H&E staining results of the lung tissue of nude mice after knockdown of JARID1D in the 22RV1 cells

### JARID1D promotes EMT by regulation of AR

Metastasis of clinical PCa cases is often caused by the deprivation of the AR signal, and the occurrence of CRPC is mainly related to the change in AR expression and the disorder of AR signal transmission [15–18]. Therefore, it is important to explore the interaction between JARID1D and AR in the invasion and metastasis of PCa. Thus, we first used the AR agonist R1881 to treat the CRPC cell 22RV1 for 72 h; the AR level was significantly ($P<0.01$) increased, whereas the change in JARID1D was not apparent (Fig. 3A). Similar results were observed in C4-2 cells (Fig. 3B). This suggested that AR did not regulate JARID1D. Therefore, we knocked down JARID1D in PCa cell line 22RV1 using a small interfering RNA reagent. AR expression decreased significantly ($P<0.05$) (Fig. 3C). The same experimental results were obtained from C4-2

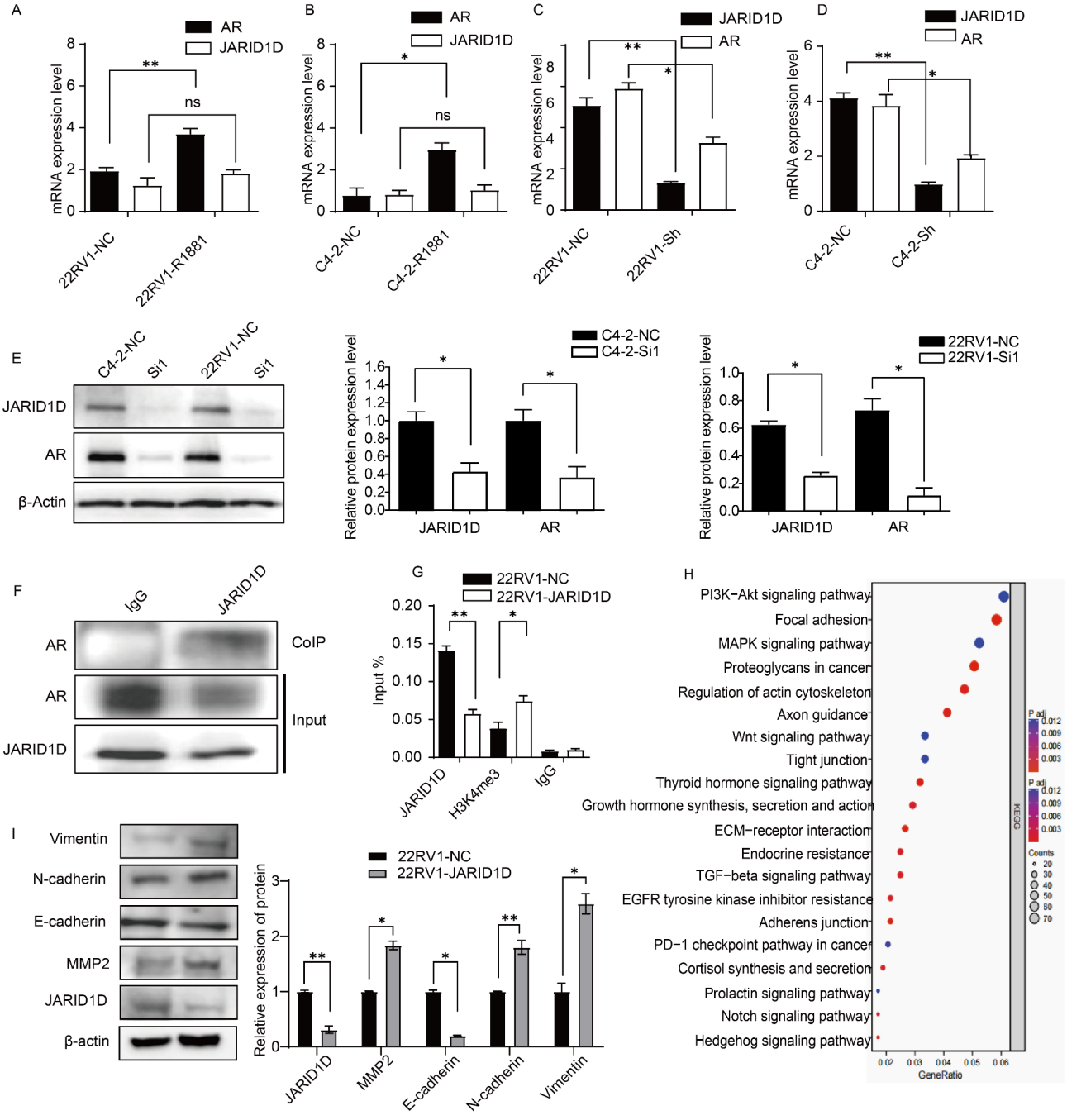


**Fig. 3** JARID1D promotes EMT by regulating AR expression. (**A-B**) mRNA expression levels of AR and JARID1D after treatment with R1881 at 22RV1 cell (**A**) and C4-2 cell (**B**) were analyzed by quantitative RT-PCR. (**C-D**) mRNA expression levels of AR and JARID1D after transfection with siRNA in 22RV1 cell (**C**) and C4-2 cell (**D**) by quantitative RT-PCR. (**E**) Western blot analysis of AR and JARID1D protein expression levels after transfection with siRNA in 22RV1cell and C4-2 cell and quantitative analysis results. (**F**) Before protein blotting with mutual antibodies, the anti-JARID1D, anti-AR, or control antibodies were used to perform Co-IP on 22RV1 cells grown in serum containing medium. (**G**) ChiP-PCR was used to analyze the effect of knocking down JARID1D in 22RV1 cells on the H3K4me3 binding level of the AR promoter binding region. (**H**) KEGG enrichment analysis of the first 50 positive correlation genes of JARID1D. (**I**) Western blot (left) and its quantification (right) analysis of the protein expression levels of Vimentin, N-cadherin, E-cadherin, and MMP2 after knocking down JARID1D in 22RV1 cells was done. EMT, epithelial-mesenchymal transition; AR, androgen receptor

cells (Fig. 3D). The results of the Western blot were also consistent with these findings (Fig. 3E), indicating that knocking down JARID1D reduces the level of AR. Therefore, JARID1D is an upstream gene of AR, and protein interaction experiments demonstrated that JARID1D could produce immune coprecipitation with AR, indicating that JARID1D can directly regulate AR (Fig. 3F).

To explore the specific mechanism by which JARID1D regulates AR transcription, we used quantitative ChIP to detect the effect of JARID1D knockdown on the AR promoter in 22RV1 cells. The results showed that the abundance of H3K4me3 in the promoter binding region of AR increased significantly after JARID1D knockdown (Fig. 3G). These results suggested that the methylation of H3K4me3 catalyzed by JARID1D mediated the transcriptional regulation of AR.

Further bioinformatics analysis was performed to explore the molecular mechanism of JARID1D promoting PCa metastasis using the PCa database (TCGA, Firehose Legacy), The top 50 genes with multiple of difference greater than 1.5 were introduced into OmicShare to analyze the KEGG pathway. The PI3K-Akt signaling pathway was the most abundant. (Fig. 3H). It is a crucial intracellular signaling pathway, playing a central role in processes such as cell survival, proliferation, and metabolism [19]. However, quantitative RT-PCR analysis showed that the knockdown of JARID1D had nearly no effect on PI3K expression (Supplementary Fig. 2). The literature reported that the Wnt signaling pathway played an important role in the development of PCa metastasis [20]. So, we investigated the relationship between JARID1D and Wnt, and found that after knocking down JARID1D in 22RV1 cells, the change of Wnt was not significant (Supplementary Fig. 3), which was consistent with the change of PI3K shown in Supplementary Fig. 2. These results indicated that both PI3K and Wnt signaling pathways did not play a dominant role in JARID1D mediated invasion and metastasis of PCa. Further analysis of the KEGG enrichment data, we found that JARID1D expression was also closely related to cell adhesion, tight junctions, cell outer membrane receptor interaction, and other genes related to cell invasion. Some studies have reported that JARID1D is closely associated with EMT-related molecules [6, 21]. Therefore, we further detected the expression of N-cadherin, E-cadherin, Vimentin and MMP2 after JARID1D knockdown and confirmed that the expression level of these EMT-related genes increased after JARID1D knockdown (Fig. 3I).

#### Curcumin improves the expression level of JARID1D and inhibits the growth and invasion of PCa

To explore the effect of curcumin on the growth of PCa cells with different phenotypes, LNCaP, 22RV1, C4-2 and PC3 cells were treated with different concentrations of curcumin for 72 h. We found that curcumin could extensively inhibit the proliferation of these four different phenotypes of PCa cells, wherein the $IC_{50}$ values were 10.58 μM, 12.65 μM, 14.49 μM and 32.64 μM, respectively (Fig. 4A). To determine the effect of curcumin on the expression of JARID1D in PCa cells, we treated these four types of cells with curcumin at different concentrations. The results exhibited that treatment with curcumin could increase the expression of JARID1D in different PCa cells in a dose-dependent manner (Fig. 4B and G). All these results suggested that curcumin increased the expression of JARID1D and suppressed the growth of PCa cells.

At the mechanism level, we found that the demethylation activity of JARID1D (Supplementary 4 Fig.A) and EMT (Supplementary 4 Fig.B) conversion were positively correlated with the concentration of curcumin. In order to further investigate the effect of curcumin-induced demethylation of JARID1D on AR and EMT-related molecules, we treated 22RV1 cells with 14 μM curcumin, which made JARID1D demethylation the most significant (Fig. 4H), and found that the expression of AR and AR promoter binding region H3K4me3 increased significantly (Fig. 4I). Then, the changes of EMT-related markers were further verified. The results showed that the expressions of MMP2, N-cadherin and Vimentin increased with the up-regulation of JARID1D after curcumin treatment, but the expression of E-cadherin changed inversely. However, in the 22RV1-shJARID1D group, after curcumin was added, JARID1D's ability to inhibit the invasion of PCa cells was restored, and the expressions of MMP2, N-cadherin and Vimentin decreased, while the expression of E-cadherin increased (Fig. 4J). Finally, the effect of demethylation of JARID1D induced by 14 μM curcumin on the invasive ability of 22RV1-JARID1D cells was studied, and it was found that the invasive ability of cells was significantly reduced (Fig. 4K). Finally, to confirm the long-lasting effect of curcumin, we induced C42 cells (CRPC) with 20 μm of enzalutamide, and after 120 d, the expression of NEPC markers (SYP, CGA) increased gradually (Supplementary 4 Fig.C). It was suggested that C42 cell induced by enzalutamide appeared NEPC phenotype, and we named this cell $C42^R$ (NEPC). Then, we treated C42 and $C42^R$ cells with 10 μm curcumin for 48 h, the results of RT-PCR showed that the cascade signal of JARID1D/AR/EMT was still present in $C42^R$ (Supplementary 4 Fig.D). These results suggested that curcumin could inhabit PCa metastasis in vitro for a long time. Therefore, we believed that curcumin could stimulate the JARID1D/AR/EMT signaling cascade through demethylation to inhibit the metastatic potential of CRPC.

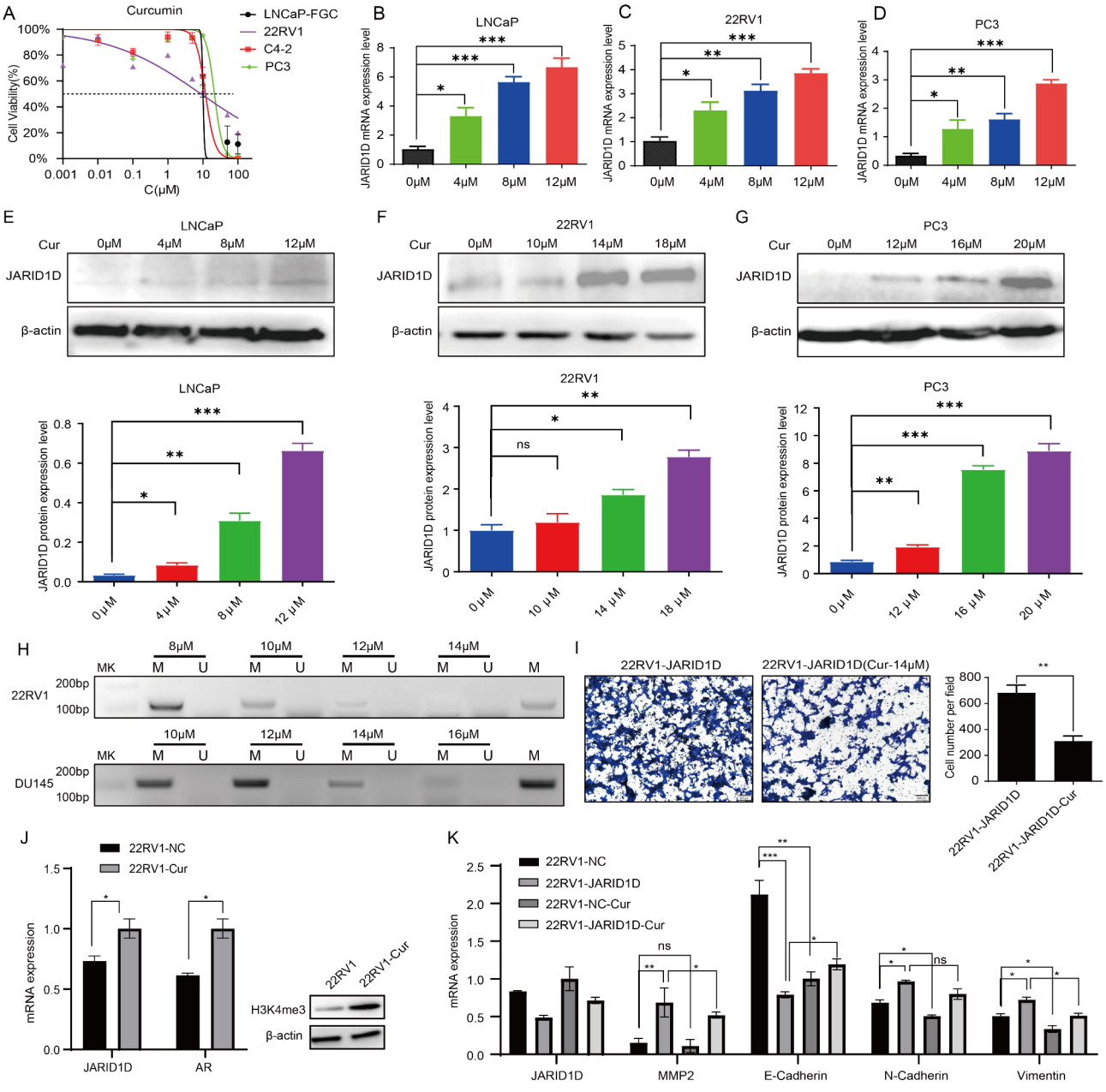


**Fig. 4** Curcumin improves the expression level of JARID1D and inhibits the growth and invasion of PCa. (**A**) The effects of curcumin on the growth of LNCaP, 22RV1, C4-2 and PC3 cells were analyzed. (**B-D**) Quantitative RT-PCR analysis of the effect of the different doses of curcumin on JARID1D mRNA expression in LNCaP, 22RV1, and PC3 cells. (**E-G**) Western blot and quantitative analysis of the effect of the different doses of curcumin on JARID1D protein expression in LNCaP, 22RV1, and PC3 cells. (**H**) The methylation status of JARID1D gene before and after curcumin treatment on 22RV1 cells. MK: DNA Marker; M: Methylation of 125 bp; U: Non methylated 125 bp; M: Positive control. (**I**) The mRNA expression of AR and H3K4me3 after 14 μM curcumin treatment. (**J**) The mRNA expression of EMT-related molecules after 14 μM curcumin treatment. (**K**) Transwell experiment (left) and its quantification (right) to analyze the changes in the invasion ability of 22RV1-JARID1D cells treated with curcumin (14 μM). Error bar represents standard deviation, $n = 3$ independent repetitions

### Curcumin inhibits PCa metastasis caused by JARID1D knockdown through EMT in AR-dependent cells

To evaluate whether curcumin can inhibit PCa metastasis in vivo, 22RV1 sh-JARID1D cells were injected into nude mice through the tail vein. A lung metastasis model was successfully established. The animal experiment was divided into a control group (vector administration, i. p.) and curcumin treatment group (30 mg/kg, i. p., thrice a week). The results showed that curcumin treatment significantly weakened the luciferase signal in the 22RV1 sh-JARID1D ($P<0.001$) cell groups (Fig. 5A), and the metastasis signal of tumors in the lungs of nude mice also

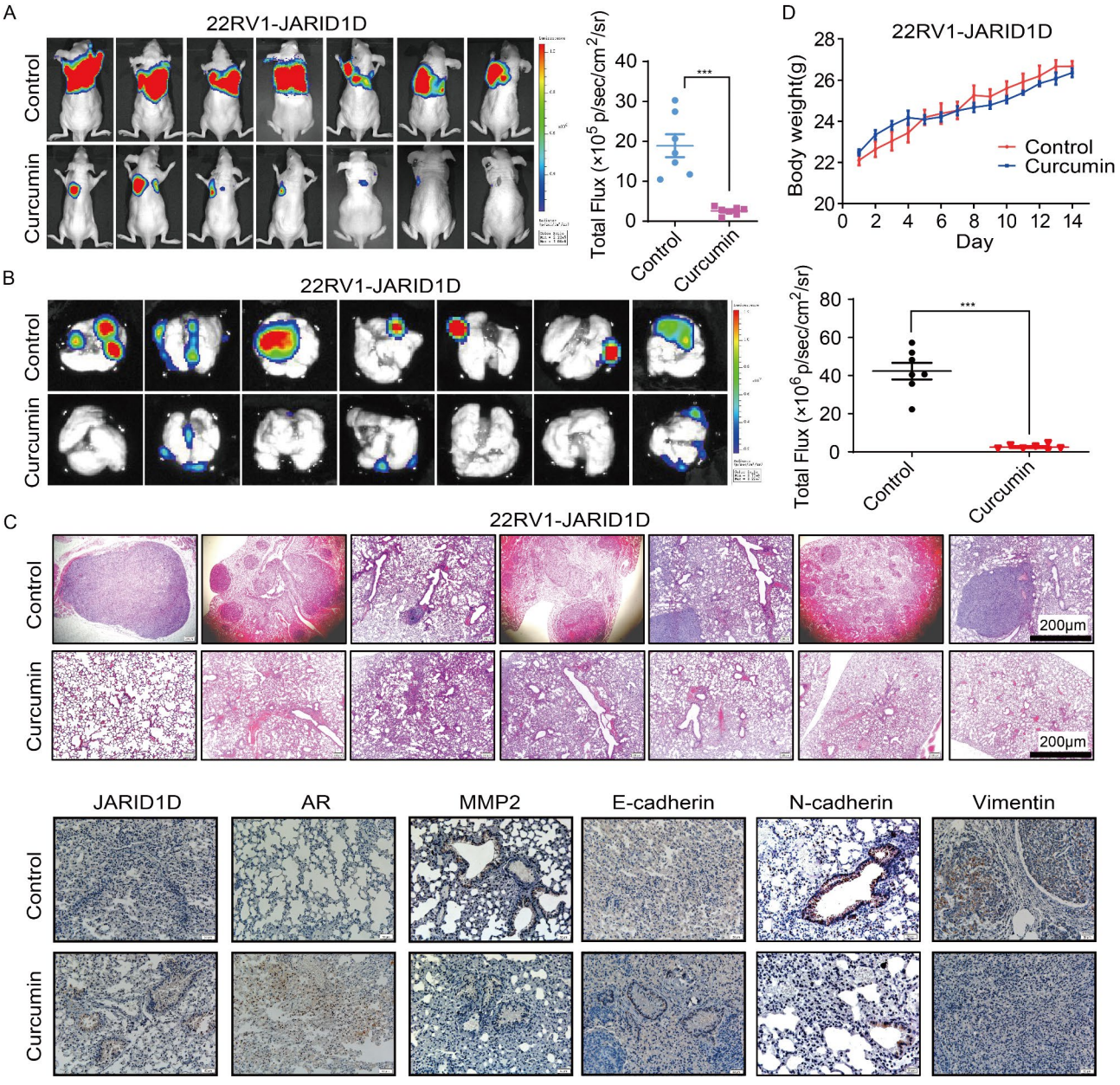


**Fig. 5** Curcumin inhibits PCa lung metastasis caused by JARID1D knockdown through EMT in AR-dependent cells in vivo. (**A-B**) Bioluminescence image (left) and its quantification (right) of (A) whole mouse and (**B**) mouse lung tissue after treatment with curcumin. (**C**) H&E staining results of the mouse lung metastasis tumor tissue after curcumin treatment. (**D**) The body weight of mice treated with curcumin was monitored every two days. (**E**) The expression level of JARID1D, AR, MMP2, E-cadherin, N-cadherin, Vimentin in the lung metastasis model induced by the injection of 22RV1-JARID1D cells after treatment with curcumin. EMT, epithelial-mesenchymal transition; PCa, prostate cancer; AR, androgen receptor

displayed a consistent trend (Fig. 5B). H&E staining confirmed that the number of tumor metastases in the lung tissue of the curcumin group was significantly lower than that in the control group (Fig. 5C). The animal weight did not display apparent differences between the curcumin and control groups (Fig. 5D), indicating that curcumin does not have apparent side effects. These results revealed that curcumin inhibited the enhancement of metastasis induced by JARID1D knockdown.

In order to explore the underlying mechanism, we established the lung metastasis models of PCa successfully by injection of 22RV1 sh-JARID1D cells. After treatment with curcumin, the expression of JARID1D, AR and E-cadherin in the lung metastatic tumor tissues was increased significantly, and the expression of N-cadherin, Vimentin and MMP2 was also decreased (Fig. 5E). In order to confirm the origin of cancer cells in the lung tissue of mice, we further validated by staining for human

CK8 (Supplementary Fig. 5). Treatment with curcumin reduced the expression of CK8. According to the report of literature [22], the decrease in CK8 expression to some extent indicates a decrease in the invasion and metastasis ability of PCa cells. Therefore, this result supported the therapeutic effect of curcumin.

It was suggested that curcumin inhibited the metastatic potential of CRPC cells by suppressing the interaction of some EMT-relative genes with JARID1D in AR-dependent cells.

## Discussion

The Y chromosome plays an important role in prostate tumor development [23], wherein 52% of patients with PCa completely or partially lack the Y chromosome [24]. This deficiency may impair the function of Y-chromosome-encoded male-specific proteins, which are crucial for curbing tumor invasion and metastasis. Among these, JARID1D stands out as a key player [6]. Driven by these insights, our study probed the potential of JARID1D as a therapeutic target against PCa invasion and metastasis. We discovered that JARID1D knockdown in CRPC cell line 22RV1 markedly boosted the invasiveness of PCa cells in vitro and promoted lung metastasis in vivo (Figs. 1 and 2). Several studies have confirmed that epigenetic regulators are closely associated with tumor invasion and metastasis. Cao et al. [25] reported that JARID1A (also called KDM5D and SMCY) promoted breast cancer progression and metastasis . Similarly, the epigenetic regulator KDM4C may promote breast tumor growth and metastasis [26]. The expression of SMYD3 was upregulated in several cancer types, which could increase MMP9 expression [27]. Conversely, the knockdown of epigenetic regulators that inhibit tumor metastasis, such as JARID1D, could promote tumor growth and metastasis. As reported, JARID1D expression is either absent or downregulated in most metastatic prostate tumors [28].

Metastases are the most common phenotype in the development of PCa and predict poor prognosis [29]. The underlying biological mechanisms of PCa metastasis remain largely elusive, but are suspected to involve the EMT signaling pathway [30]. In this study, bioinformatics analysis showed that the signaling molecules related to JARID1D were mainly enriched in cell adhesion signaling pathways (Fig. 3H). The expression levels of EMT-related regulatory factors, such as N-cadherin, Vimentin and MMP2, were significantly increased when JARID1D was knocked down (Fig. 3I). Elevated levels of these proteins were also observed in lung metastatic tumor tissues, implicating the intensified EMT, due to JARID1D suppression, as a pivotal factor in PCa metastasis (Fig. 5). Advanced PCa frequently experiences AR signal loss, triggering the EMT and facilitating metastasis [31]. Our findings corroborate this link, showing that JARID1D knockdown in AR-dependent CRPC cells, specifically 22RV1, downregulates AR expression, intensifies EMT, and propels metastatic progression (Figs. 2 and 3). This suggests the potential of JARID1D agonists in curbing PCa spread. Despite the absence of specific agonists for JARID1D, we have opted for multi-target agents, including Chinese herbal medicine, to maximize therapeutic effectiveness.

Curcumin, a promising anti-cancer agent, has garnered significant interest for its ability to modulate multiple signaling pathways, thereby inhibiting the proliferation, migration, and invasion of PCa cells [32]. Our investigation revealed that curcumin effectively suppressed the growth of 22RV1 cells at an $IC_{50}$ of 12.65 μM and enhanced both the expression and demethylation activity of JARID1D at a 14 μM dose (Fig. 4C and F). This suggests a capacity of curcumin to upregulate JARID1D expression through demethylation, concurrent with its growth inhibitory effect on PCa cells. Notably, while curcumin at 12 μM induced high JARID1D expression in PC3 cells, with an $IC_{50}$ of 32.64 μM, this concentration did not impede their growth (Fig. 4D and G). These observations indicate that curcumin's influence on JARID1D expression may not directly correlate with its growth inhibitory action in all PCa cell contexts. Curcumin can affect the progression of PCa through the PI3K and Wnt signaling pathways [33, 34], but it is more related to the growth and proliferation of PCa cells. In JARID1D mediated invasion and metastasis of PCa, the PI3K and Wnt signaling pathways do not play a dominant role. (Supplementary Fig. 2, Supplementary Fig. 3)

Both previous report and our study confirm that curcumin may has a DNA demethylation effect on tumor cells [9]. Further experiments demonstrated that curcumin could significantly inhibit the proliferation of PCa cells with different phenotypes (LNCaP, 22RV1, C4-2, and PC3). This action not only reverses the methylation state of these cells but also upregulates JARID1D expression, suggesting curcumin's role as an epigenetic modulator of AR and EMT markers, thereby inhibiting PCa metastasis (Fig. 4). In addition, we selected PCa cells at different stages and found that the JARID1D/AR/EMT cascade signal persisted after curcumin was administered. In vitro evidence was provided for the possible persistence of curcumin (Supplementary Fig. 4C-D). We further selected AR-dependent PCa cells (22RV1) to develop a lung metastasis model of PCa and found that treatment with curcumin significantly inhibited PCa metastasis caused by JARID1D knockdown and decreased the expression of N-cadherin, Vimentin and MMP2, but stimulated the expression of JARID1D, AR and E-cadherin (Fig. 5). These results highlight curcumin's potential to impede PCa invasion and metastasis,

particularly when JARID1D is compromised, through the regulation of AR/EMT pathways.

In summary, although curcumin has shown certain anti-cancer effects in vitro and animal models, further investigation is required to understand its long-term impact and bioavailability in humans [35, 36]. Future research needs to focus on improving the bioavailability of curcumin and exploring its long-term mechanisms of action in the human body. Furthermore, the exact molecular basis and complex signaling pathways involved still need to be elucidated. For instance, further research is warranted to understand how curcumin targets and potentially ameliorates the tumor microenvironment [37]. In addition, the dose of curcumin used in the study may be different in clinical application, so it is necessary to further study its efficacy and safety at different doses. Furthermore, the administration strategy of curcumin combined with JARID1D agonist may be more beneficial to inhibit PCa metastasis.

## Conclusion

JARID1D expression is significantly diminished in advanced prostate cancer (PCa), contributing to tumor metastasis and migration. Our study revealed that the epigenetic modifier JARID1D could restrict the progression of PCa, and curcumin could stimulate the expression level of JARID1D and regulate the transcriptional regulation of AR through demethylation. Upregulation of JARID1D was observed to suppress EMT in addition to restraining tumor growth and metastasis. Taken together, these findings provide the evidence that curcumin has therapeutic potential for invasive PCa, and targeting JARID1D may be a viable therapeutic strategy, particularly in metastatic prevention.

### Abbreviations

| | |
|---|---|
| PCa | prostate cancer |
| AR | androgen receptor |
| CRPC | castration-resistant prostate cancer |
| EMT | epithelial-mesenchymal transition |
| FMMU | The Fourth Military Medical University |
| Co-IP | co-immunoprecipitation |
| IHC | immunohistochemistry |
| MSP | methylation-specific PCR |
| NEPC | neuroendocrine prostate cancer |

## Supplementary Information

The online version contains supplementary material available at https://doi.org/10.1186/s12935-024-03483-2.

Supplementary Material 1

### Acknowledgements

We are grateful to Dr. Leland W. K. Chung (Cedars-Sinai Medical Center, Los Angeles, CA, USA) for kindly providing the method of animal experiments.

### Author contributions

Conceptualization, X.Q.; Validation, H.Y and Z.C.; methodology, Z.C., Q.J. and Z.Y.; formal analysis, A.Q; investigation, Z.J.; writing-original draft preparation, S.C.; visualization, S.C.; funding acquisition, S.C. All authors have read and agreed to the published version of the manuscript.

### Funding

The work was supported by the National Natural Science Foundation of China (32070532 and 32270566) and Shaanxi Province Innovation Capability Support Plan (2022PT-38).

### Data availability

No datasets were generated or analysed during the current study.

## Declarations

### Informed consent

Not applicable.

### Competing interests

The authors declare no competing interests.

### Author details

[1]Division of Cancer Biology, Laboratory Animal Center, The Fourth Military Medical University, Xi'an 710032, Shaanxi, China
[2]Animal Experiment Center, Guangzhou University of Chinese Medicine, Guangzhou 510405, China
[3]Gansu University of Chinese Medicine, Lanzhou 730030, China
[4]National Demonstration Center for Experimental Preclinical Medicine Education, The Fourth Military Medical University, Xi'an 710032, China

Received: 18 June 2024 / Accepted: 14 August 2024
Published online: 01 September 2024

### References

1. Ashrafizadeh M, Paskeh MDA, Mirzaei S, et al. Targeting autophagy in prostate cancer: preclinical and clinical evidence for therapeutic response. J Exp Clin Cancer Res. 2022;41(1):105. https://doi.org/10.1186/s13046-022-02293-6.
2. Shigeta K, Kosaka T, Hongo H, et al. Castration-resistant prostate cancer patients who had poor response on first androgen deprivation therapy would obtain certain clinical benefit from early docetaxel administration. Int J Clin Oncol. 2019;24(5):554–6. https://doi.org/10.1007/s10147-018-01388-5.
3. Berish RB, Ali AN, Telmer PG, Ronald JA, Leong HS. Translational models of prostate cancer bone metastasis. Nat Rev Urol. 2018;15(7):403–21. https://doi.org/10.1038/s41585-018-0020-2
4. Chen X, Liu J, Cheng L, et al. Inhibition of noncanonical wnt pathway overcomes enzalutamide resistance in castration-resistant prostate cancer. Prostate. 2020;80(3):256–66. https://doi.org/10.1002/pros.23939.
5. Isensee J, Witt H, Pregla R, et al. Sexually dimorphic gene expression in the heart of mice and men. J Mol Med (Berl). 2008;86(1):61–74. https://doi.org/10.1007/s00109-007-0240-z.
6. Li N, Dhar SS, Chen TY, et al. JARID1D is a suppressor and prognostic marker of prostate cancer invasion and metastasis. Cancer Res. 2016;76(4):831–43. https://doi.org/10.1158/0008-5472.
7. Nakamura K, Yasunaga Y, Segawa T, et al. Curcumin down-regulates AR gene expression and activation in prostate cancer cell lines. Int J Oncol. 2002;21(4):825–30. PMID: 12239622.
8. Fabianowska-Majewska K, Kaufman-Szymczyk A, Szymanska-Kolba A, et al. Curcumin from turmeric rhizome: a potential modulator of DNA methylation machinery in breast cancer inhibition. Nutrients. 2021;13(2):332. https://doi.org/10.3390/nu13020332.
9. Ming T, Tao Q, Tang S, et al. Curcumin: an epigenetic regulator and its application in cancer. Biomed Pharmacother. 2022;156:113956. https://doi.org/10.1016/j.biopha.2022.113956.
10. Contreras-Sanzón E, Prado-Garcia H, Romero-Garcia S, et al. Histone deacetylases modulate resistance to the therapy in lung cancer. Front Genet. 2022;13:960263. https://doi.org/10.3389/fgene.2022.960263. Published 2022 Oct 3.

11. Mahmoudi Z, Jahani M, Nekouian R. Role of curcumin on miR-26a and its effect on DNMT1, DNMT3b, and MEG3 expression in A549 lung cancer cell. J Cancer Res Ther. 2023;19(7):1788–93. https://doi.org/10.4103/jcrt.jcrt_2181_21.
12. Li X, Huo C, Xiao Y, et al. Bisdemethoxycurcumin protection of cardiomyocyte mainly depends on Nrf2/HO-1 activation mediated by the PI3K/AKT pathway. Chem Res Toxicol. 2019;32(9):1871–79. https://doi.org/10.1021/acs.chemrestox.9b00222.
13. Ibanez de Caceres I, Cortes-Sempere M, Moratilla C, et al. IGFBP-3 hypermethylation-derived deficiency mediates cisplatin resistance in non-small-cell lung cancer. Oncogene. 2010;29(11):1681–90. https://doi.org/10.1038/onc.2009.454.
14. Katta S, Srivastava A, Thangapazham RL, et al. Curcumin-gene expression response in hormone dependent and independent metastatic prostate cancer Cells. Int J Mol Sci. 2019;20(19):4891. https://doi.org/10.3390/ijms20194891.
15. Larsson PF, Karlsson R, Sarwar M, et al. FcγRIIIa receptor interacts with androgen receptor and PIP5α to promote growth and metastasis of prostate cancer. Mol Oncol. 2022;16(13):2496–2517. https://doi.org/10.1002/1878-0261.13166.
16. Li Q, Liu B, Chao HP, et al. LRIG1 is a pleiotropic androgen receptor-regulated feedback tumor suppressor in prostate cancer. Nat Commun. 2019;10(1):5494. https://doi.org/10.1038/s41467-019-13532-4.
17. Sharma NL, Massie CE, Ramos-Montoya A, et al. The androgen receptor induces a distinct transcriptional program in castration-resistant prostate cancer in man. Cancer Cell. 2013;23(1):35–47.https://doi.org/10.1016/j.ccr.2012.11.010.
18. Chen H, Zhou L, Wu X, et al. The PI3K/AKT pathway in the pathogenesis of prostate cancer. Front Biosci (Landmark Ed). 2016;21(5):1084–1091. Published 2016 Jun 1.
19. Wang Q, Li W, Zhang Y, et al. Androgen receptor regulates a distinct transcription program in androgen-independent prostate cancer. Cell. 2009;138(2):245–56. https://doi.org/10.1016/j.cell.2009.04.056.
20. Li N, Li Y, Lv J, et al. ZMYND8 reads the dual histone mark H3K4me1-H3K14ac to antagonize the expression of metastasis-linked genes. Mol Cell. 2016;63(3):470–84. https://doi.org/10.3389/fonc.2019.00131.
21. Cheaito KA, Bahmad HF, Hadadeh O, et al. EMT markers in locally-advanced prostate cancer: predicting recurrence?. Front Oncol. 2019;9:131. https://doi.org/10.3389/fonc.2019.00131.
22. Yao L, Ren S, Zhang M, et al. Identification of specific DNA methylation sites on the Y-chromosome as biomarker in prostate cancer. Oncotarget. 2015;6(38):40611–621. https://doi.org/10.18632/oncotarget.6141.
23. Kaplan Z, Zielske SP, Ibrahim KG, et al. Wnt and β-catenin signaling in the bone metastasis of prostate cancer. Life (Basel). 2021;11(10):1099. https://doi.org/10.3390/life11101099.
24. Yao L, Ren S, Zhang M, et al. Identification of specific DNA methylation sites on the Y-chromosome as biomarker in prostate cancer. Oncotarget. 2015;6(38):40611–40621. https://doi.org/10.18632/oncotarget.6141.
25. Patel R, Khalifa AO, Isali I, et al. Prostate cancer susceptibility and growth linked to Y chromosome genes. Front Biosci (Elite Ed). 2018;10(3):423–36. https://doi.org/10.2741/e830.
26. Luo W, Chang R, Zhong J, et al. Histone demethylase JMJD2C is a coactivator for hypoxia-inducible factor 1 that is required for breast cancer progression. Proc Natl Acad Sci USA. 2012;109:E3367–76. https://doi.org/10.1073/pnas.1217394109
27. Cao J, Liu Z, Cheung WK, et al. Histone demethylase RBP2 is critical for breast cancer progression and metastasis. Cell Rep. 2014;6:868–77. https://doi.org/10.1016/j.celrep.2014.02.004.
28. Cock-Rada AM, Medjkane S, Janski N, et al. SMYD3 promotes cancer invasion by epigenetic upregulation of the metalloproteinase MMP-9. Cancer Res. 2012;72:810–20. https://doi.org/10.1158/0008-5472.CAN-11-1052.
29. Wu PC, Lu JW, Yang JY, et al. H3K9 histone methyltransferase, KMT1E/SETDB1, cooperates with the SMAD2/3 pathway to suppress lung cancer metastasis. Cancer Res. 2014;74:7333–43. https://doi.org/10.1158/0008-5472.
30. Zhang XH, Jin X, Malladi S, et al. Selection of bone metastasis seeds by mesenchymal signals in the primary tumor stroma. Cell. 2013;154(5):1060–73. https://doi.org/10.1016/j.cell.2013.07.036.
31. Lochter A, Galosy S, Muschler J, et al. Matrix metalloproteinase stromelysin-1 triggers a cascade of molecular alterations that leads to stable epithelial-to-mesenchymal conversion and a premalignant phenotype in mammary epithelial cells. J Cell Biol. 1997;139:1861–72. https://doi.org/10.1083/jcb.139.7.1861.
32. Shanmugam MK, Rane G, Kanchi MM, et al. The multifaceted role of curcumin in cancer prevention and treatment. Molecules. 2015;20(2):2728–69. https://doi.org/10.3390/molecules20022728.
33. Lim SC, Geleta B, Maleki S, et al. The metastasis suppressor NDRG1 directly regulates androgen receptor signaling in prostate cancer. J Biol Chem. 2021;297(6):101414. https://doi.org/10.1016/j.jbc.2021.101414.
34. Abd Wahab NA, Lajis NH, Abas F, et al. Mechanism of anti-cancer activity of curcumin on androgen-dependent and androgen-independent prostate cancer. Nutrients. 2020;12(3):679. https://doi.org/10.3390/nu12030679.
35. Gupta SC, Patchva S, Aggarwal BB. Therapeutic roles of curcumin: lessons learned from clinical trials. AAPS J. 2013;15(1):195–218. https://doi.org/10.1208/s12248-012-9432-8.
36. Abd El-Hack ME, El-Saadony MT, Swelum AA, et al. Curcumin, the active substance of turmeric: its effects on health and ways to improve its bioavailability. J Sci Food Agric. 2021;101(14):5747–762. https://doi.org/10.1002/jsfa.11372.
37. Mirzaei S, Paskeh MDA, Okina E, et al. Molecular landscape of LncRNAs in prostate cancer: a focus on pathways and therapeutic targets for intervention. J Exp Clin Cancer Res. 2022;41(1):214. https://doi.org/10.1186/s13046-022-02406-1.


## Publisher's note